Digest Journal of Nanomaterials and Biostructures Vol. 8, No. 1, January - March 2013, p. 117- 126

# NANOTECHNOLOGICAL APPROACH FOR EXPLORING THE ANTIBIOFILM A POTENTIAL OF AN ETHANOMEDICINAL HERB *ANDROGRAPHIS PANICULATA* FOR CONTROLLING LUNG INFECTION CAUSING *PSEUDOMONAS AERUGINOSA*

KASI MURUGAN[a*], SELVANAYAKI KRISHNASAMY[b], V.B.KALYANASUNDARAM[b], SALEH AL-SOHAIBANI [a]

[a]*Department of Botany & Microbiology, College of Science, King Saud University, Riyadh, Saudi Arabia*

[b]*P.G. and Research Department of Microbiology, K.S.R. College of Arts and Science, Tiruchengodu, India*

Nanotechnology finds immense application in drug development and its targeted delivery. The growth and biofilm inhibitory potential of silver nanoparticles (AgNPs), synthesized by the ethanomedicinal herb *Andrographis paniculata* antibiofilm extract against cystic fibrosis, isolate *Pseudomonas aeruginosa* by using the biofilm specific methods carried out. AgNps were synthesized by a rapid biological method using *A. paniculata* antibiofilm extract as a reducing agent. UV–Vis spectroscopy and TEM (Transmission electron microscopy) analysis was carried out to confirm and characterize AgNPs. Phytochemical constituents were determined by GC-MS analysis. The dose dependent antibacterial activity based on the well diffusion and modified quantitative spectrophotometric microtiter plate method were used for *in vitro* anti-biofilm assay. The structure of GC-MS identified phytochemicals exposed the silver reducing diverse functional groups availability. The synthesized particles were 50nm diameter spheres and their thin faint exotic material layer due to phytochemicals interaction, likely explains the stability of AgNPs. AgNPs were found to impede *P. aeruginosa* exopolysaccharide and biofilm synthesis. Synthesised AgNPs treatment resulted in more than 90% biofilm formation inhibition. The *in vitro* biofilm inhibition demonstrated the therapeutic potential of *A. paniculata* antibiofilm activity and their phytochemical drug lead's novel application which may be a surrogate to antibiotics.

(Received November 11, 2012; Accepted December 20, 2012)

*Keywords:* Biofilms; COPD; Cystic fibrosis; Exopolysaccharide; Pathogenesis

## 1. Introduction

Nanotechnology is a rapidly growing interdisciplinary area of science and technology that integrates materials science and biology [1]. There is an immense interest in biomedicine applications of nanoparticles owing to their size and structural similarity with biological molecules. Antibiotic evasion by multidrug resistant bacteria and the almost negligible discovery rate of novel antibiotics has forced the exploration of possible alternatives. Establishment of a bacterial infection as a biofilm, a complex three-dimensional, attached bacterial community, protects the bacteria from therapeutic agents and host defences, with potentially devastating consequences for patient morbidity and mortality [2]. Biofilms are implicated in over 80 % of bacterial infections as well as treatment related infections in the body [3]. The protection offered by biofilms arises from multiple mechanisms, including a greater number of persistent cells, quorum sensing systems, biosorption, gene expression response and efflux systems. Limited mass

*Corresponding author: murutan@gmail.com

diffusive transport within biofilms also stifles the action of antimicrobials. Other advantageous facets of biofilm living include an altered microenvironment with different levels of metabolic activity, and spatial heterogeneity of antimicrobial resistance gene expression by the microbial cells within [4].

*Pseudomonas aeruginosa* is a Gram-negative, opportunistic bacterium responsible for several acute and chronic infections in humans, animals, insects, nematodes, and plants. It has been extensively studied as a model biofilm organism [5]. It's biofilms are also implicated in the pathogenesis of acute and chronic lung infections [3] including chronic obstructive pulmonary disease (COPD), cystic fibrosis (CF) and ventilation–associated pneumonia. Since their respiratory system mucociliary clearance is impaired, COPD and cystic fibrosis patients are vulnerable to infection by biofilm-forming bacterial pathogens as mucus accumulates in the respiratory airways, providing a nutrient-rich environment ideal for biofilm growth [6]. COPD is the fourth-leading cause of death globally, affecting more than fifty million people. Excess health-care expenditures are estimated at nearly $6,000 annually for every COPD patient in the United States[7]. CF is believed to affect approximately 70,000 people worldwide, although in some developing countries the disease is not always diagnosed [8]. CF is a common autosomal recessive disorder in the Caucasian population, affecting 1 in 2000 of live births. It affects the epithelial lining of major organs, particularly the lungs, with the majority of mortalities caused by pulmonary complications [9].

Antibiotic inhalation therapy is an ideal treatment for these biofilm related lung infections, being readily available and of low systemic toxicity. Solutions containing the antibiotics are typically delivered directly to lung infection sites by nebulisation. The thick mucus layer (i.e. sputum) and the EPS matrix, however, act as physical barriers that limit access of inhaled antibiotics to the biofilm cells, resulting in poor antibacterial efficacy. The primary mechanism of this inhibition is binding between the antibiotic molecules and the sputum contents, which limits antibiotic diffusion. Consequently, the nebulized antibiotic delivery can only effectively target biofilm assemblages at the periphery of the sputum [6]. Although current prophylactic anti-inflammatory and antibacterial chemotherapy has dramatically increased the life span of CF patients, the development of novel therapeutic modalities is warranted [10]. In particular, there is an urgent need for novel therapeutic agents that can effectively penetrate both newly forming and established biofilms. Harnessing the unique properties of nanoparticles to target infection and especially to control highly challenging biofilm-mediated diseases, has motivated an upsurge in research on their novel inhibitory activity, eco-friendly synthesis, and synergistic action with other therapeutic agents.

Todoroff and Vanbever [11] comprehended that nanomedicines deposited in the lung largely escape uptake by lung-surface macrophages and can remain there for weeks, without significant translocation across respiratory epithelia. Hence, development of nanoparticles that can be introduced to the lung via aerosol delivery represents an exciting frontier in pharmaceutical design [9]. Antibiotic-loaded nanoparticle inhalation can therefore provide an attractive alternative to standard lung biofilm infection therapy [6]. However, the requisite of 50 to 500 times higher minimal inhibitory concentration of antibiotics than that required for planktonic free-floating forms [12] enhances the risk of resistance development. This risk has raised growing concern over the use of antibiotic alternate agents.

New sources, especially from the rich repertoire of the plant kingdom, are being investigated as control agents against many types of pathogens. Earlier investigations, however, have almost exclusively focused on planktonic bacteria with little emphasis on the more antimicrobial resistant pathogens and intractable biofilm forms[13]. To identify potential therapeutic agents and targets of biofilm-forming opportunistic pathogens, much research has focused on the model biofilm-forming opportunistic pathogen *P. aeruginosa* [2]. Previously, we identified the biofilm forming cystic fibrosis isolates *Pseudomonas aeruginosa* KMS P03 and *P. aeruginosa* KMS P05. These multidrug resistant strains are susceptible to extracts of *Andrographis paniculata*. In particular, *A. paniculata* disrupts growth and biofilm formation of both strains, possibly by interfering with cell attachment [14]. The traditional medicinal plant *A. paniculata* thus presents as a promising agent for reducing microbial colonization on tissue surfaces and epithelial mucosa in CF patients. The therapeutic use of these plants is expected to

increase as a result. In the present work, we synthesized silver nanoparticles (AgNPs) from *A. paniculata* extracts and investigated their *in vitro* antibiofilm activity which may lead to the synthesis and delivery of a novel antibiofilm agent.

## 2. Materials and Method

### 2.1 Organisms used

The biofilm-forming *Pseudomonas aeruginosa* KMS P03 (which causes acute pulmonary infection in CF patients) and *P. aeruginosa* KMS P05 were obtained from culture collections at P.G. & Research Department of Microbiology, K.S.R College of Arts and Science, Tiruchengode, India. The isolated biofilms forming ability and antibiotic resistance were described earlier [14]. Isolates were maintained on blood agar plates for sub-culturing at weekly intervals.

### 2.2 Plant collection and preparation of Andrographis paniculata extracts

The whole plant *A. paniculata* (Fig 1) was collected from the Erode district and its surroundings (latitude 10° 36' – 11° 58' north; longitude 76° 49' – 77° 58' east)**,** Tamil Nadu, India. The adhering soil particles were removed by repeated washing with deionised water and the plant materials were shadow-dried and powdered. Bioactive components from 25g of ground plant samples were extracted with 250ml of methanol; the extract was concentrated under reduced pressure at 40°C and stored at 4°C for later processing. The bacterial growth inhibitory and antibiofilm activity of the extracts were reaffirmed [14].

*Fig 1. The flowering plant Andrographis paniculata[14]*

### 2.3 Silver nano particles synthesis using *A. paniculata* extract

For the synthesis of silver nanoparticles (AgNPs), the rapid biological method as described in [15] was followed. Silver salt precursor silver nitrate ($AgNO_3$) (AR grade) was procured from E-Merck, Mumbai, India. 1Mm aqueous $AgNO_3$ was prepared and aged in amber glass reagent bottles for three 158 days to allow the system to equilibrate. Typically, 10ml of the *A. paniculata* extract was added to 19ml of 1mM $AgNO_3$ solution. AgNPs were synthesized at $25^0$C to $95^0$C with reflux. This reaction was carried out for 24 to 48 hours. The resulting deep yellow-brown in colour solution indicating the presence of metallic silver was monitored. The formed AgNPs was purified by repeated centrifugation at 15,000rpm for 20min and the pellet was dispensed in

deionized water. Quantitative monitoring of concentration of AgNPs was determined by getting 2 peak values at 390 and 430nm respectively. Peak values obtained at 430nm indicate the conversion of silver nitrate to metallic silver. Sample images were obtained by transmission electron microscopy (JEOL JSM –169 5600 LV, Sastra University, Thanjore, Tamilnadu, India) operated at 120 kV. The volume and molar concentration of AgNPs was calculated using the following

$$N = \frac{\Pi}{6}\frac{\rho D3}{M} = 30.89602D^{3}$$

(Where N =number of atoms per nanoparticles; Π = 3.14; ρ =density of face centred, cubic (fcc) silver =10.5g/cm$^3$; D =average diameter of nanoparticles =50nm; M = atomic mass of silver =107.868g; NA =number of atoms per mole (Avogadro's number) = 6.023 X $10^{23}$).

**2.4 Determination of antibiofilm activity of synthesized silver nanoparticles**

The concentration of synthesised nanoparticles required for biofilm-formation inhibition was determined by dose dependent antibacterial activity, based on the well diffusion method. 20ml of Congo red agar containing brain heart infusion broth (37g/l, sucrose 0.8g/l, agar-agar 10g/l), and Congo red stain (0.8g/l) [16] were poured into sterile Petri plates. The Congo red stain was prepared and autoclaved separately as a concentrated aqueous solution, and added to the media when the agar had cooled to 55°C. The plates were inoculated with 16-18h-old *Pseudomonas* cultures with turbidity adjusted to 0.5 McFarland standards by swapping with a cotton swab. Wells (6 mm diameter) were punched in the agar with a cork borer and filled with 25 µl of nanoparticle solutions at different concentrations (10-100mM). The plates were incubated at 37° C for 18-24 h.

The modified quantitative spectrophotometric microtiter plate method [17] was used to assay the activity of the synthesized AgNPs. The selected isolates were inoculated into sterile trypticase soy broth and incubated at 37°C for 24h. 20ml of each culture was then added to 180ml trypticase soy broth. From these mixtures, 200µl samples were added to each row of microtiter plate and incubated at 37°C for 24-48h. After incubation, the samples were replaced with 50µl of 60Mm AgNPs suspended in deionized water. At this concentration, the nanoparticles inhibit exopolysaccharide synthesis but the organism remains viable. Positive and negative control wells were constructed by inoculation with bacterial broth culture and tobramycin (50µg/ml), respectively. Following incubation at 37°C for 48h, wells were emptied and stained with 0.1% crystal violet solution for 5min, then rinsed with sterile distilled water four times to remove unutilized media, nanoparticles and planktonic cells. The absorbances of the wells were determined at 490nm using a micro plate reader (model 680, Bio-Rad, Hercules, CA). From the OD values, organism stability was assessed by coefficient of variation, and the efficacy of silver particles was estimated [17] by percentage of reduction, defined as follows

$$\text{Percentage reduction} = \frac{(C-T)-(B-T)}{(C-T)} \times 100$$

**2.5 GC-MS analysis of Plant Extract**

Bioactive component analyses of the methanol extract were undertaken by GC-MS. Analyses were performed in a PerkinElmer Clarus 500 coupled to a Clarus 500 Mass Spectrometer mass detector under electron impact ionization (70 eV). The interface temperature was 280°C and the MS scan range was 40-450 atomic mass units (AMU). For chromatography, a capillary column Elite-5ms (5%Phenyl 95% dimethylpolysiloxane; length 30m, inner diameter 250µm, film thickness 0.25 µm) was used. The stepped up temperature program was implemented as follows: held at 70°C for 10 min, followed by temperature raise from 70 to 150°C at a rate of 10°C/min (5min), then to 280°C at 8°C/min. Helium was used as carrier gas injected at 1ml/min; injection volume 1µl. The solvent, delayed by 2 min, was injected in a split ratio of 1:10. Peaks of the individual constituents were referred to the mass spectral database in the Wiley NIST reference

library, to establish their identity.

## 3.Results

Biofilm-specific investigation techniques confirmed the biofilm forming capacity and the multidrug-resistant nature of both *Pseudomonas aeruginosa* KMS P03 and *P. aeruginosa* KMS P05. The results provide strong rationale for designing intervention strategies against these organisms. Here we have adopted the rapid biological synthesis method for silver nanoparticles coated with highly bioactive extract of medicinal plant *A. paniculata*. The synthesized nanoparticles were characterized by UV–Vis spectroscopy and visualized under TEM. Reduction of silver ions and formation of nanoparticles is apparent when the solution becomes brown-yellow. Spectra of such solutions exhibited a single peak maximum absorption at 420nm indicating the presence of nanometer-sized AgNPs. Even after 10 times dilution, the absorption spectrum of the diluted silver nanoparticle solution was almost identical to that of the original solution, confirming that the solution was stable. Shape and size distributions of the nanoparticles were determined from the SEM images (Fig 1). Silver nanoparticles were generally found to be spherical with a mean diameter of 50nm. The regular size and shape of the nanoparticles suggests that the aggregation is driven by specific interactions rather than by random processes. More precise observations revealed a thin, faint layer of exotic material surrounding the silver nanoparticles, presumably comprising organic matter from the *A. paniculata* extract. Nanoparticle concentration was calculated as 3837233.003 silver atoms per nanoparticle (assuming that all silver ions were incorporated into nanoparticles, yielding 260nM molar concentration of the nanoparticle solution).

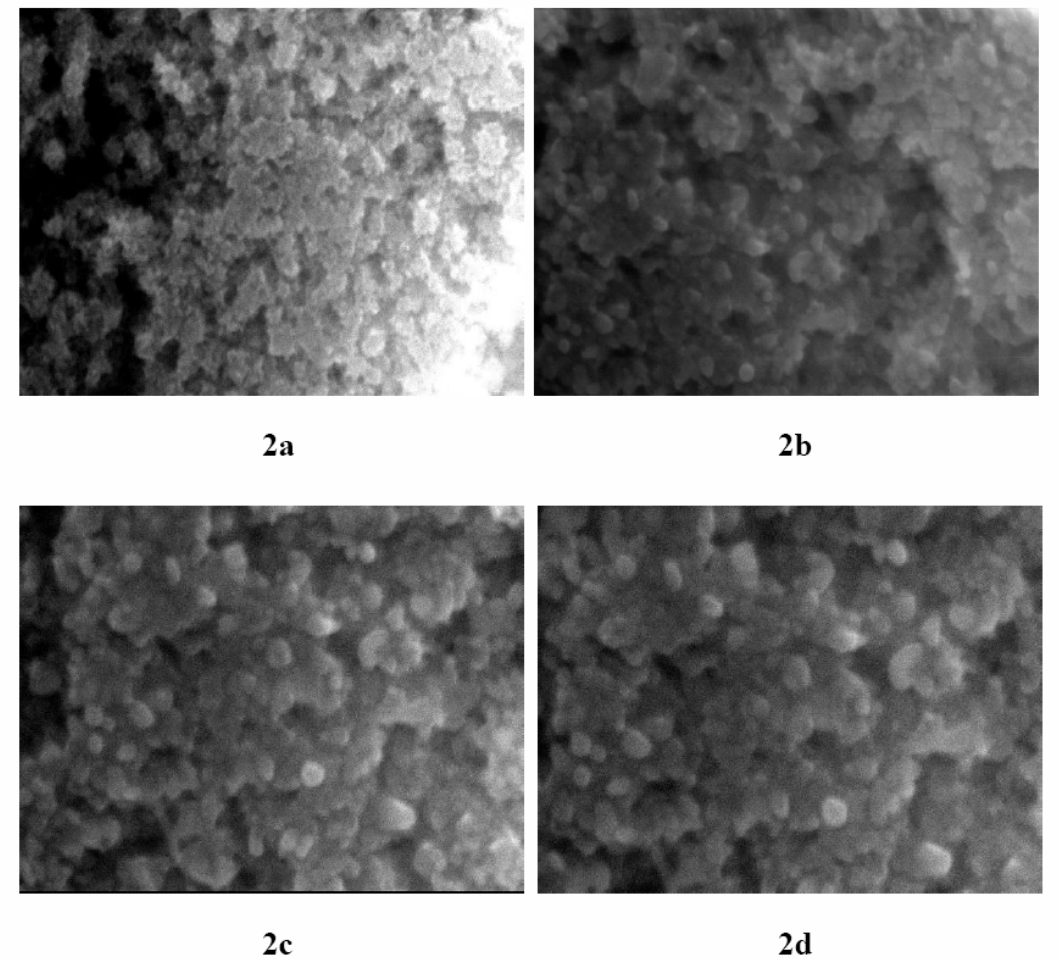


*Fig. 2. TEM micrograph 2a(25K); 2b (50K); 2c(60K); 2d(75K) of silver nanoparticles synthesized by the reaction of 1mM silver nitrate with A.paniculata antibiofilm extract.*

GC–MS measurements of *A. paniculata* methanolic extract (Table 1) enabled the identification of 32 components. Among the phytochemicals, Pyran-4-one, 3,5-dihydroxy-6-methyl-2,3-dihydropyran-4-one, (4Z)-4-((E)-but-2-enylidene)-3,5,5-trimethylcyclohex- 2-en-1-one, 3,7,11,15-Tetramethyl2-hexadecen-1-ol (Phytol); hexadecanoic acid; 4H-1-Benzopyran-4-one, 5-Hydroxy-6,7-dimethoxy-2-phenyl- are found in large quantities along with several compounds present in minor proportions. The relative percentage of these phytochemicals, their chemical structures, and their contributing important functional groups (obtained from PubMed) were determined. The presence of wide diversity functional groups for silver reduction was revealed. These compounds are suggested to mediate the metal ion reduction process, and may also control the stability of formed nanoparticles by coating them and hindering agglomeration.

*Table 1: Compounds identified GC-MS analysis of antibiofilm methanol extract of A. paniculata, their structure, retention time and relative abundance.*

| S.No. | Peak Name | 2D/3D Structure | Retention time | % Peak area |
|---|---|---|---|---|
| 1) | Maltol<br>Formula: $C_6H_6O_3$ |  | 6.40 | 0.8970 |
| 2) | 4H-Pyran-4-one, 2,3-dihydro-3,5-dihydroxy-6-methyl-<br>Formula: $C_6H_8O_4$ |  | 7.47 | 3.0891 |
| 3) | Benzene, (ethenyloxy)-<br>Formula: $C_8H_8O$ |  | 8.55 | 0.3380 |
| 4) | Methanecarbothiolic acid<br>Formula: $C_2H_4OS$ |  | 8.93 | 0.0494 |
| 5) | Phenol, 5-methyl-2-(1-methylethyl)-, acetate, Formula: $C_{12}H_{16}O_2$ |  | 9.76 | 0.1831 |
| 6) | 4-Hydroxy-2-methylacetophenone<br>Formula: $C_9H_{10}O_2$ |  | 10.31 | 0.1514 |
| 7) | 4-Hydroxy-6-methylpyrazolo[3,4-d]pyrimidine<br>Formula: $C_6H_6N_4O$ | 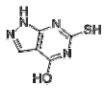 | 10.33 | 0.0814 |
| 8) | à-D-Mannopyranoside, methyl 3,6-anhydro-<br>Formula: $C_7H_{12}O_5$ | 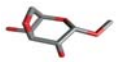 | 13.60 | 1.1229 |
| 9) | Benzoic acid, 2-methyl-<br>Formula: $C_8H_8O_2$ |  | 14.06 | 0.0611 |
| 10) | Phenol, 2-pentyl-<br>Formula: $C_{11}H_{16}O$ |  | 15.29 | 1.0102 |
| 11) | 2(4H)-Benzofuranone, 5,6,7,7a-tetrahydro-4,4,7a-trimethyl-, (R)-<br>Formula: $C_{11}H_{16}O_2$ |  | 16.36 | 0.1752 |
| 12) | (-)-R-Phenethanamine, 1-methyl-N-vanillyl-<br>Formula: $C_{17}H_{21}NO_2$ |  | 16.85 | 0.1653 |
| 13) | 1,2,3,5-Cyclohexanetetrol, (1à,2á,3à,5á)-<br>Formula: $C_6H_{12}O_4$ | | 18.17 | 24.4938 |
| 14) | Megastigmatrienone<br>Formula: $C_{13}H_{18}O$ | 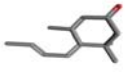 | 18.26 | 1.2454 |

| S.No. | Peak Name | 2D/3D Structure | Retention time | % Peak area |
|---|---|---|---|---|
| 15) | Pyrazine, 2,5-dimethyl-<br>Formula: $C_6H_8N_2$ | 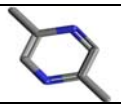 | 18.58 | 0.1202 |
| 16) | 3-Methylbut-2-enoic acid, 4-cyanophenyl ester<br>Formula: $C_{12}H_{11}NO_2$ |  | 18.93 | 0.0855 |
| 17) | Methyl acetyllithofellate<br>Formula: $C_{23}H_{40}O_5$ |  | 19.39 | 0.0397 |
| 18) | 1,6-Anhydro-2,4-dideoxy-á-D-arabo-hexopyranose:Formula: $C_6H_{10}O_3$ | | 19.77 | 1.5455 |
| 19) | 4-((1E)-3-Hydroxy-1-propenyl)-2-methoxyphenol;<br>Formula: $C_{10}H_{12}O_3$ | 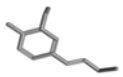 | 20.37 | 0.2198 |
| 20) | Phenol, 5-(1,5-dimethyl-4-hexenyl)-2-methyl-, (R)-<br>Formula: $C_{15}H_{22}O$ | 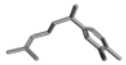 | 20.42 | 2.257 |
| 21) | n-Hexadecanoic acid<br>Formula: $C_{16}H_{32}O_2$ |  | 20.49 | 0.2134 |
| 22) | 5,5,8a-Trimethyl-3,5,6,7,8,8a-hexahydro-2H-chromene<br>Formula: $C_{12}H_{20}O$<br>MW: 180 | - | 21.19 | 0.0188 |
| 23) | 2,3-Diaminophenol<br>Formula: $C_6H_8N_2O$ |  | 21.20 | 0.1365 |
| 24) | 3,7,11,15-Tetramethyl-2-hexadecen-1-ol<br>Formula: $C_{20}H_{40}O$ | 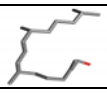 | 21.63 | 22.647 |
| 25) | Tridecanoic acid, methyl ester<br>Formula: $C_{14}H_{28}O_2$ |  | 22.94 | 0.2944 |
| 26) | n-Hexadecanoic acid<br>Formula: $C_{16}H_{32}O_2$ |  | 23.50 | 5.3245 |
| 27) | Eicosanoic acid, ethyl ester<br>Formula: $C_{22}H_{44}O_2$ | 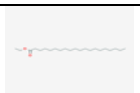 | 23.85 | 0.2825 |
| 28) | Ethanamine, 2,2'-oxybis[N,N-dimethyl-<br>Formula: $C_8H_{20}N_2O$ |  | 27.35 | 0.6526 |
| 29) | Carbamic acid, N-phenyl-, 2-methylphenyl ester<br>Formula: $C_{14}H_{13}NO_2$ |  | 27.57 | 0.1000 |
| 30) | Ethanone, 1-(4-hydroxy-3,5-dimethoxyphenyl)-<br>Formula: $C_{10}H_{12}O_4$ | 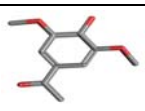 | 30.34 | 0.1481 |
| 31) | 4H-1-Benzopyran-4-one, 5-hydroxy-6,7-dimethoxy-2-phenyl-<br>Formula: $C_{17}H_{14}O_5$ | - | 33.09 | 32.1088 |
| 32) | 6H-Dibenzo(b,d)pyran-1-ol, 3-hexyl-7,8,9,10-tetrahydro-6,6,9-trimethyl-<br>Formula: $C_{22}H_{32}O_2$ | 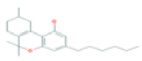 | 36.92 | 0.7739 |

Wells inoculated with AgNPs concentrations up to 30mM produced very small inhibition zones (< 5mm) on solid substrate. Surrounding colonies were reddish-black with a rough, dry, and crystalline consistency suggestive of slime production. 40 – 60mM inoculants produced a hazy zone (10mm) of pinkish red, smooth colonies with a darkening at the centre, indicating slime production inhibition. Wells inducing large inhibitory zones (> 11mm) also suppressed total growth and are thought to equally inhibit biofilm formation. When nanoparticles are present at high levels their diffusion through the medium inhibits bacterial growth by more than 90%. Cessation of biofilm formation is presumed synonymous with arrest of exopolysaccharide synthesis. Up to 60mM of AgNPs significantly arrested biofilm formation without affecting viability, whereas 70mM inhibited the growth of the organism itself (table 2). This demonstrates that AgNPs can impede exopolysaccharide synthesis and can hence interfere with biofilm formation.

*Table 2: The inhibitory activity of synthesized silver nanoparticles on the growth and biofilm formation of Pseudomonas aeruginosa isolates*

| **S. No** | **AgNP Concentration (µM)** | **Growth and biofilm inhibitory activity** | | | | | |
|---|---|---|---|---|---|---|---|
| | | *P.aeruginosa* KMS P03 | | | *P.aeruginosa* KMS P05 | | |
| | | Zone of inhibition (mm) and nature of | Nature of colony and EPS inhibition | Percentage of biofilm inhibition | Zone of inhibition | Nature of colony and EPS inhibition | Percentage of biofilm inhibition |
| **1** | Control | 0 | black No EPS inhibition | - | 0 | Reddish black No EPS inhibition | - |
| **2** | 10-40 | <5±0. 7 Hazy | Reddish black No significant EPS inhibition | ND | <5±0. 7 Hazy | Reddish black No significant EPS inhibition | ND |
| **3** | 40-50 | 6-10 Hazy | Pinkish red Moderate EPS inhibition | ND | 6-10 Hazy | Pinkish red Moderate EPS inhibition | ND |
| **4** | 60 | <11 Hazy | Pink Significant EPS inhibition | 99.04 | <11 Hazy | Pink Significant EPS inhibition | 98.23 |
| **5** | 70-100 | <11 Clear | No growth | - | <11 Clear | No growth | - |

The effect of AgNPs concentration on biofilm inhibition was established by 96 well microtiter plate assays. Concentrations high enough to inhibit exopolysaccharide synthesis but not organism viability, reduced microtiter biofilm by 99%. The precision of this result was assessed by coefficient of variation, a measure of the stability of the organisms exposed to nanoparticles. Furthermore, antimicrobial activity was markedly decreased in nanoparticle-removed (vehicle control) solutions, revealing that the role of AgNPs in antimicrobial activity.

## 4. Discussion

The ‘king of bitters’, *Andrographis paniculata* Nees (Acanthaceae), is a well-known herb whose extract possesses anti-inflammatory, antiviral, immune-stimulatory, hypoglycemic,

hypotensive and anticancer properties [18]. It has been widely used in Asia for over two thousand years to treat respiratory and urinary infections, rheumatoid arthritis, laryngitis, diarrhea, and diabetes. More recently, the benefits of *A. paniculata* extract as treatment for cold- and influenza-like illnesses have been reported in clinical studies [19]. Our present research investigates the possibility of exploiting the bioactive leaf extract to biosynthesize AgNPs. Furthermore, the results indicates the increasing the therapeutic value of this medicinally important plant resource.

In *P. aeruginosa* infection, destruction of established biofilm is one of the biggest hurdles of successful treatment. Once a biofilm has formed, the bacteria within are protected from the patient's immune system and are less susceptible to drug treatments [19]. Our earlier research revealed that the biofilm-forming cystic fibrosis isolates *Pseudomonas aeruginosa* KMSP03 and *P. aeruginosa* KMS P05 are remarkably resistant to most of the currently used antibiotics. They are, however, susceptible to *A. paniculata* extracts, among which methanol is highly effective [14]. GC-MS analysis of *A. paniculata* methanol extract uncovered over 34 bioactive components spanning various groups, which can account for the plants' effectiveness in traditional medicine and its enhanced antibiofilm activity against cystic fibrosis isolates.

The 'green chemistry' approach using plant broths is an efficient route for the synthesis of pure nanomaterials. In recent years, plant-mediated biological nanoparticle synthesis was preferred due to its simplicity and eco-friendliness [20]. However, an exact mechanism for such biosynthesis is not yet elucidated (although several hypothetical mechanisms have been proposed). During extracellular synthesis, the biomolecules act as reducing agents and the heterocyclic compounds act as capping agents for the nanoparticles [21]. Presumably, silver nanoparticle synthesis with *A. paniculata* is not an enzyme-mediated process since it proceeds under haste microwave treatment. Various components could participate in sugar reduction; namely, reducing sugars (aldoses) and ketones[22], carbohydrates and proteins [23], functional groups such as –C–O–C, –C–O–, –C=C–, and –C=O– derived from several heterocyclics[24;25], terpenoids [22] and flavonoids [26;27]. Synthesized AgNPs show signs of capping by organic molecules, consistent with numerous previous reports on plant-extract-mediated synthesized nanoparticles. Among the documented capping compounds are several plant phytochemicals such as quercetin [28], verbascoside [29], and terpenoids [30]. In our current study, diterpenoids such as andrographolide might act as capping compounds, but this proposal has yet to be confirmed.

Silver has been used as an antimicrobial agent, either as ionic species or as colloidal particles, long before the advent of antibiotics. Silver antimicrobials also have many advantages over antibiotics[31]. Since AgNPs synthesised with medicinal plant extracts can specifically target biofilms, there is opportunity for their further application against intractable pathogens. In this study we observed the concentration-dependent inhibition of growth and biofilm formation by bioengineered nanoparticles. We demonstrated that *P. aeruginosa* is significantly suppressed at AgNPs concentrations as low as 40Mm AgNP, comparable to results of previous studies. The high biofilm inhibitory activity of AgNPs might arise from the synergism between the nanoparticle and its capping plant compounds. Although the synthesized AgNPs antagonize cystic fibrosis causatives by specifically targeting their important virulence factor (i.e. their biofilm-forming capacity), they remain void for medical applications until sufficient toxicity data are available. Other applications of green synthesized AgNPs include formulation of potential antibacterial agents and control of device-related infections and spoilage. The identification and characterization of plant bioactive nanoparticle capping compounds, and knowledge of how the nanoparticles will behave *in vivo*, as well as biofilm models, are required before AgNPs can be developed into a medically and commercially significant antibiofilm agent.

From the results obtained here, we conclude that an effective novel antibiofilm agent can be formulated by combining the antimicrobial potential of medicinal plants with nanotechnological applications. Further isolation and activity determination of the identified compounds can result in potential drug leads against biofilm mediated infections.

**Acknowledgement**

The authors extend their appreciation to the Deanship of Scientific Research at King Saud University for funding the work through the research group project No RGP-VPP-183.

## References


[1] K.K. Panda, V.M.M. Achary, R. Krishnaveni, B.K. Padhi, S.N. Sarangi, S.N. Sahu, B.B. Panda. Toxicol. In Vitro **25**, 1097 (2011).
[2] L.M. Junker, J.Clardy. Antimicrob. Agents Chemother. **51**, 3582 (2007).
[3] J.Fricks-Lima, C.M.Hendrickson, M.Allgaier, H.Zhuo, J.P.Wiener-Kronish, S.V.Lynch, K.Yang. Int. J. Antimicrob. Agents **37,** 309 (2011).
[4] O.Choi, C.P.Yu, G.E.Ferna´ndez, Z.Hu. Water Res. **44**, 6095 (2010).
[5] C.Attila, A.Ueda, T.K.Wood. Appl. Microbiol. Biotechnol. **78**, 293 (2008).
[6] K. Kho, W.S.Cheow, R.H.Lie, K. Hadinoto. Powder Technol. 2**03**, 432 (2010).
[7] CDC. 2000—2005. MMWR **57**, 1229 (2008).
[8] F.Ratjen, F. Brockhaus, G. Angyalosi. J. Cystic Fibrosis **8**, 361 (2009).
[9] R.Osman, P.L.Kan, G.Awad, N.Mortada, A.E.El-Shamy, O.Alpar. Int. J. Pharm. **408,** 257 (2011).
[10] M.Alipour, Z.E.Suntres, M. Halwani, A.O.Azghani, A.Omri. PLoS ONE **4**, e5724 (2009).
[11] J.Todoroff, R.Vanbever. Curr. Opin. Colloid Interface Sci. **16**, 246 (2011).
[12] H. Anvar, M.K.Dasgupta, J.W.Costerton. Antimicrob. Agents Chemother**. 34**, 2043 (1990).
[13] M.Sandasi, C.M.Leonard, A.M.Viljoen. Lett. Appl. Microbiol. **50**, 30 (2010).
[14] K.Murugan, K.Selvanayaki, S.A.Sohaibani. World J. Microbiol. Biotechnol**. 27,** 1661(2011).
[15] J.Y. Song, B.S.Kim. Bioprocess Biosyst. Eng**. 32**, 79-84 (2009).
[16] D.J.Freeman, F.R. Falkiner, C.T. Keane. J. Clin. Pathol. **42**, 872 (1989).
[17] B.Pitts, M.A.Hamilton, N. Zelver, P.S.Stewart. J. Microbiol. Methods **54**, 269 (2003).
[18] S.R. Jada, A.S.Hamzah, N.H.Lajis, M.S.Saad, M.F.G.Stevens, J.Stanslas. J. Enzyme Inhib. Med. Chem. **21**, 145 (2006).
[19] X.Jiang, P.Yu, J.Jiang, Z. Zhang, Z.Wang, Z.Yang, Z.Tian, S.C.Wright, J.W. Larrick, Y.Wang. Eur. J. Med. Chem**. 44**, 2936 (2009).
[20] G.S.Ghodake, N.G.Deshpande, Y.P.Lee, E.S.Jin. Colloids Surf. B: Biointerfaces **75**, 584 (2010).
[21] N.Durán, P.D.Marcato, M.Durán, A.Yadav, A.Gade, M.Rai. Appl. Microbiol. Biotechnol**. 90**, 1609 (2011).
[22] S.S.Shankar, A. Ahmad, A.Rai, M.Sastry. J. Colloid Interface Sci. **275**, 496 (2004).
[23] A.Richardson, B.C. Chan, R.D.Crouch, A. Janiec, B.C.Chan, R.D.Crouch. Chem Educ **11**, 331 (2006).
[24] J.Huang, C.Chen, N. He, J. Hong, Y.Lu, L. Qingbiao, W.Shao, D.Sun, X.H.Wang, Y.Wang, X.Yiang. Nanotechnology **18**, 105 (2007).
[25] K.K. Panda, A.B.Das, B.B.Panda. Genetic Resour. Crop Evol. **56**, 629 (2009).
[26] D.Raghunandan, S.Basavaraja, B.Mahesh, S.D.Balaji, S.Y.Manjunath, A.Venkataraman. Nanobiotechnology **5**, 34 (2009).
[27] R.W. Raut, J.R. Lakkakula, N.S.Kolekar, V.D.Mendhulkar, S.B.Kashid. Curr. Nanosci. **5**, 117 (2009).
[28] A.Nahrstedt, M.Hungeling, F. Peterit. Fitoterapia **77**, 484 (2006).
[29] D.Cruz, P.L.Falé, A. Mourato, P.D.Vaz, M.L.Serralheiro, A.L.Lino. Colloids Surf. B: Biointerfaces **81**, 67 (2010).
[30] J.Y Song, E.Y.Kwon, B.S.Kim. Bioprocess Biosyst. Eng. **33**, 159 (2010).
[31] C.Y.Flores, C.Diaz, A.Rubert, G.A.Benítez, M.S.Moreno, M.A.Fernández Lorenzo de, R.C.Salvarezza, P.L.Schilardi, C.Vericat. J. Colloid Interface Sci. **350**, 402 (2010).